Metastable self-trapping of positrons in MgO

M. A. Monge, R. Pareja, and R. González
Departamento de Física, Universidad Carlos III de Madrid, C/Butarque 15, 28911 Leganés, Spain

Y. Chen
U.S. Department of Energy, ER 131, Division of Materials Sciences, Office of Basic Energy Sciences, Washington, D.C. 20874-1290
(Received 10 July 1996)

Low-temperature positron annihilation measurements have been performed on MgO single crystals containing either cation or anion vacancies. The temperature dependence of the *S* parameter is explained in terms of metastable self-trapped positrons which thermally hop through the crystal lattice. The experimental results are analyzed using a three-state trapping model assuming transitions from both delocalized and self-trapped states to deep trapped states at vacancies. The energy level of the self-trapped state was determined to be (62 ± 5) meV above the delocalized state. The activation enthalpy for the hopping process of self-trapped positrons appears to depend on the kind of defect present in the crystals. [S0163-1829(97)09001-2]

I. INTRODUCTION

Positron annihilation spectroscopy (PAS) is a sensitive probe to investigate vacancy-like defects and the electronic distribution in metals and semiconductors. In ionic materials positron annihilation experiments are difficult to interpret because of the variety of interactions that a thermalized positron can experience in an ionic lattice. Combination of theoretical work and experiments are necessary to understand the behavior of positrons in these materials. Oxide crystals with a simple crystalline structure are suitable media to explore positron behavior in ionic crystals. Positron lifetime spectra in some of these oxides are simple enough to be decomposed into one or two components, without a long-lived component attributable to positronium (Ps) state. These results are in contrast with those observed in complex oxides and alkali halides, where the formation of Ps states is common and their lifetime spectra are complex. The results in simple oxides are interpreted in terms of delocalized and trapped positron states, as it is commonly done in metals and semiconductors. Calculations based on this scheme agree with experimental data.[1] In MgO single crystals, the theoretical bulk lifetime for positrons is 167 ps,[1] in excellent agreement with the experimental value of (166 ± 3) ps.[2]

Optical absorption and luminescence experiments, in conjunction with PAS, have previously been used to investigate positron trapping at well-characterized defects in MgO. It has been demonstrated that positronium hydride (PsH) and Ps states can be formed in thermochemically reduced hydrogen doped MgO crystals.[3,4] Low-temperature positron annihilation experiments in MgO crystals, with or without hydride ions, are expected to give valuable information on positron annihilation characteristics in ionic crystals based on temperature dependence of positron trapping.

In the present study, low-temperature Doppler-broadening and lifetime experiments were performed on high quality MgO single crystals containing either impurity-compensated cation vacancies, or anion vacancies. In Doppler-broadening measurements, the temperature dependence of the line shape parameter *S* is explained if self-trapped positrons, which move through the lattice by thermal hopping, such as small polarons, are considered. In alkali halides, evidence for metastable self-trapped positronium formation has been reported[5–7] as well as positron annihilation models based on polaron states.[8,9] However, this particular annihilation scheme has not been investigated in simple oxides.

II. EXPERIMENTAL METHOD

The high purity MgO single crystals used were grown by the arc-fusion technique at the Oak Ridge National Laboratory. The total impurity content is estimated to be <100 ppm.[10] Thermochemical reduction (TCR) of the crystals was performed at 2400 K in 7 atmospheres of magnesium vapor in a tantalum chamber followed by rapid cooling.[11,12] Subsequent heat treatments of the TCR samples were made inside a graphite container inserted in a horizontal furnace with flowing high-purity nitrogen. Optical measurements were made with a Perkin-Elmer 2000 FT-IR Spectrophotometer (far infrared), and a Perkin-Elmer Lambda 19 Spectrophotometer.

Doppler-broadening measurements over the temperature range $10-300$ K were carried out with the pair of samples mounted inside a closed He cycle cryostat with the positron source sandwiched between the samples. A ^{22}Na positron source sealed between thin kapton foils was used. The annihilation radiation was recorded with a stabilized Ge detector having an energy resolution of 1.62 keV at the 1.33 MeV line of ^{60}Co. The Doppler-broadening of the 511 keV annihilation peak was characterized in terms of the line shape parameter *S*. This is defined as the count fraction in a 1.39 keV window centered at the annihilation peak.

Lifetime measurements were made between $100-300$ K with the samples mounted in a liquid-nitrogen flow cryostat. A spectrometer with a time resolution (FWHM) of 235 ps was used.

III. RESULTS AND DISCUSSION

A. As-grown crystals

In this section, using Doppler-broadening experiments, we first considered the possibility that in as-grown MgO

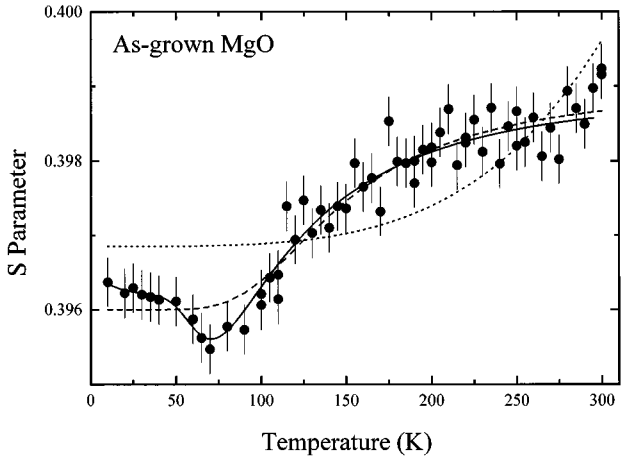

FIG. 1. Parameter S versus temperature for as-grown MgO crystals. The resulting fits assuming (a) only lattice thermal expansion, (b) metastable self-trapping of positrons, and (c) self-trapping and positron trapping at defects, are represented by dotted, dashed, and solid lines, respectively.

crystals the observed temperature dependence of the parameter S is due to either lattice thermal expansion, or to metastable self-trapped positron states. Secondly, complementary experiments are made to determine the mean positron lifetime and its variation with temperature.

Figure 1 shows the variation of the parameter S with temperature. After an initial decline between 10 and 75 K, the S parameter increased with temperature. In order to check if the observed temperature dependence was due to thermal expansion of the lattice, an attempt was made to fit the experimental points to the following equation[13]

$$S(T)=S_0\exp\left(\int_{T_0}^{T}\delta\beta(T)dT\right), \tag{1}$$

where $\delta=V/S(\partial S/\partial V)_P$ is the coefficient that gives the magnitude of the volume effect on the parameter S, $\beta(T)=1/V(\partial V/\partial T)_P$ is the volume thermal expansion coefficient and T_0 is the lower measuring temperature. Here V is the volume, T the temperature and P the pressure. Using for $\beta(T)$ the data reported in Ref. 14 for MgO, assuming δ independent of T, and taking δ and S_0 as adjustable parameters, the best adjusted curve is the dotted line shown in Fig. 1. It is clear that the observed temperature dependence could not be attributed to thermal expansion effect.

Next, the possibility of a metastable self-trapped positron state with an energy ϵ above the free positron ground state is considered. The free positron state is a delocalized polaron-like state, also called large polaron, and the metastable self-trapped state is a small polaron-like state. The transition from a delocalized state to a self-trapped state is controlled by acoustic phonon coupling. The positron can be localized between two adjacent anion sites in the MgO lattice creating a self-trapped state similar to a self-trapped hole, i.e., a V_k center, in alkali and metal halides and in alkaline earth fluorides.[15] The positron fractions f_f in the delocalized state and f_{st} in the self-trapped state are, respectively, given by[5,16]

$$f_f(T)=\frac{1}{1+AT^{-3/2}\exp\left(-\frac{\epsilon}{kT}\right)}, \tag{2}$$

$$f_{st}(T)=[1-f_f(T)]=\frac{1}{1+A^{-1}T^{3/2}\exp\left(\frac{\epsilon}{kT}\right)}, \tag{3}$$

where k is the Boltzmann constant and A a numerical parameter satisfying $AT^{-3/2}\gg 1$.

The parameter S can be described by

$$S(T)=f_f(T)S_f+f_{st}(T)S_{st}, \tag{4}$$

where S_f and S_{st} are the S values for delocalized and self-trapped states, respectively. Using S_f, S_{st}, A, and ϵ as adjustable parameters, the dashed curve shown in Fig. 1 is the best fit of Eq. (4) to the experimental points. The corresponding values are $(S_{st}-S_f)=(2.95\pm0.06)\times10^{-3}$, $A=(4.4\pm0.3)\times10^5$ K$^{3/2}$, and $\epsilon=(70\pm7)$ meV. It is clear that this model does not satisfactorily fit the experimental points for $T<120$ K.

Next, positron trapping at defects was considered. In as-grown MgO crystals, we know that there exist several impurity-compensated cation vacancies (V-type centers), mainly V_{OH}^-, V_{Al}^-, and V_{F}^- centers due to the inherent presence of hydrogen, aluminum, and fluorine, respectively.[17] Their linear configurations are correspondingly:

$$\mathrm{Mg^{2+}-OH^{-}-[Mg]-O^{2-}-Mg^{2+}}$$

$$\mathrm{Al^{3+}-O^{2-}-[Mg]-O^{2-}-Mg^{2+}}$$

$$\mathrm{Mg^{2+}-F^{-}-[Mg]-O^{2-}-Mg^{2+}}.$$

Here [Mg] refers to a magnesium vacancy. These defects are negatively charged with respect to the lattice and are strong positron traps.[2,18] The atomic concentration was estimated to be $\sim10^{-6}$.[17] If a hole is in the vicinity of each of the above defects, its likely trapping site would be the $\mathrm{O^{2-}}$ ion adjacent to the [Mg], away from the impurity charge compensator, thus forming an $\mathrm{O^-}$ ion.

Assuming positron trapping at V-type centers, three different positron states are considered: (i) delocalized or large polaron states, (ii) self-trapped or small polaron states, and (iii) trapped states at V-type centers. Positron trapping at V-type centers was observed at room temperature;[2,18] at this temperature, the probability for the positron to be in a self-trapped state is very high. Thus, transitions from both free and self-trapped states to trapped states are included. The model to fit the experimental points is depicted in Fig. 2. The mathematical expressions for this model are derived in the Appendix. With the above assumptions the parameter S is given by

$$S(T)=P_f(T)S_f+P_{st}(T)S_{st}+P_v(T)S_v, \tag{5}$$

where $P_f(T)$, $P_{st}(T)$, and $P_v(T)$ are the temperature-dependent fraction of positrons annihilating in delocalized, self-trapped, and trapped state, respectively, and S_f, S_{st}, and S_v the values of S for the respective states. $P_f(T)$, $P_{st}(T)$, and $P_v(T)$ are given by Eqs. (A11). The

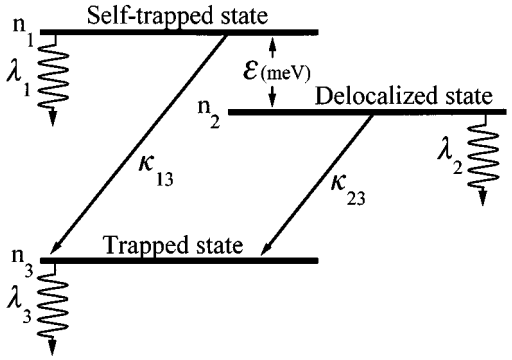

FIG. 2. Positron state scheme in MgO containing either cation or anion vacancies.

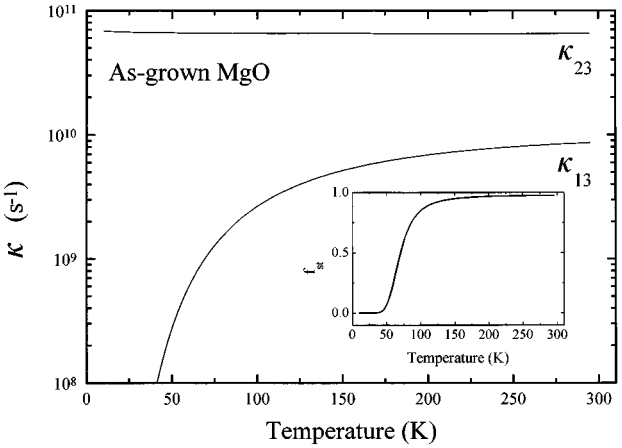

FIG. 3. Trapping rates κ_{13} and κ_{23} versus temperature for as-grown MgO crystals. The inset shows the variation of the self-trapped positron fraction with temperature.

temperature dependence of P_f, P_{st}, and P_v are described by the constants ϵ, A, ΔE, a, b, and c introduced in Eqs. (3), (A14), (A15), and (A17).

The experimental values of the S parameter are fitted to Eq. (5) with S_f, S_{st}, S_v, λ_1, λ_2, and the constants which give the temperature dependence of P_f, P_{st}, and P_v as adjustable parameters; λ_1 and λ_2 are the annihilation rate for self-trapped and delocalized states, respectively. The solid curve in Fig. 1 shows the best fit. It describes very well the temperature dependence of S. The values of the adjustable parameters are given in Table I. From the values of ϵ, A, ΔE, a, b, and c, the positron trapping rates from self-trapped κ_{13} and from delocalized states κ_{23}, as well as the positron fraction in self-trapped states f_{st} can be obtained by means of Eqs. (A15), (A17), and (3). Figure 3 shows the temperature dependence of κ_{13}, κ_{23}, and f_{st}. The trapping rate κ_{23} appears to be essentially temperature independent.

Figure 4 depicts the fraction of positrons annihilated in each state, P_f, P_{st}, and P_v, predicted by Eqs. (A11), as a function of the temperature. Below 40 K, there is no self-trapping, $P_{st}=0$. Further, 90% of the annihilated positrons were in trapped states at V-type defects, $P_v=0.9$, and the remainder in delocalized states, $P_f=0.1$. Above 40 K, P_v drops steeply to a minimum at 95 K while the fraction of positrons annihilated in self-trapped states, P_{st}, rises to a maximum. P_{st} is higher than P_v in the temperature interval 75−155 K. At room temperature 60% of the positrons annihilate at V-type defects and the remainder annihilate in self-trapped states. Above ~170 K no positrons annihilate in delocalized states ($P_f=0$).

The lifetimes of delocalized positrons, $\tau_f=\lambda_2^{-1}$, and self-trapped positrons, $\tau_{st}=\lambda_1^{-1}$, can be determined from the fitting of Eq. (5); see Table I. The resulting mean value of $\tau_{st}=(169\pm4)$ ps is in agreement with the lifetime value of (166 ± 3) ps previously reported for positrons annihilated in the bulk at room temperature.[2,18] For τ_f a mean value of (133 ± 12) ps is obtained.

The positron lifetime spectrum in the temperature range 100−300 K appears to be single component and temperature independent, resulting in an observed lifetime between 173

TABLE I. Values of the adjustable parameters for as-grown and TCR MgO crystals. The values of the parameter A are $(12.0\pm0.4)\times10^5$ $K^{3/2}$ and $(7.3\pm0.2)\times10^5$ $K^{3/2}$ for the as-grown and TCR samples, respectively.

		TCR samples			
	As-grown		Annealed		
	samples	as-TCR	5 min 1370 K	10 min 1370 K	10 min 1470 K
C_v (at^{-1})	$[V^-]\sim10^{-6}$	$[F]\sim5\times10^{-6}$	$[F]\sim4\times10^{-7}$	$[F]\sim2\times10^{-7}$	$[F]=1.8\times10^{-7}$
$\lambda_1^{-1}=\tau_{st}$ (ps)	167±4	166±5	171±2	170±3	172±4
$\lambda_2^{-1}=\tau_f$ (ps)	131±17	135±4	134±16	130±12	135±6
$(S_v-S_f)\times10^2$	5.62±0.06	6.79±0.04	6.80±0.14	6.2±0.4	6.77±0.06
$(S_v-S_{st})\times10^2$	0.81±0.03	5.31±0.09	5.30±0.08	5.4±0.6	5.32±0.07
ϵ (meV)	55±7	65±6	66±3	60±5	62±4
ΔE (meV)	22±2	50±8	51±2	55±10	52±2
a ($\times10^8 s^{-1}$)	5.7±0.6	3.4±0.5	1.90±0.15	1.64±0.06	1.4±0.2
b ($\times10^9 s^{-1}$)	67.1±1.5	–	–	–	–
c ($\times10^9 s^{-1}$)	26±7	–	–	–	–
d ($\times11^{12}$ s^{-1})	–	~23	~13	~13	~11
e ($\times10^9 s^{-1}$)	–	2.81±0.03	1.57±0.06	1.35±0.04	1.21±0.07

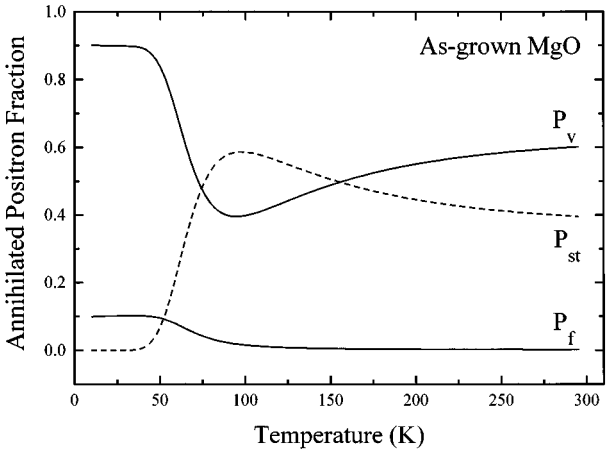

FIG. 4. Fractions of positrons annihilating in delocalized P_f, self-trapped P_{st}, and trapped state P_v, versus temperature for as-grown MgO.

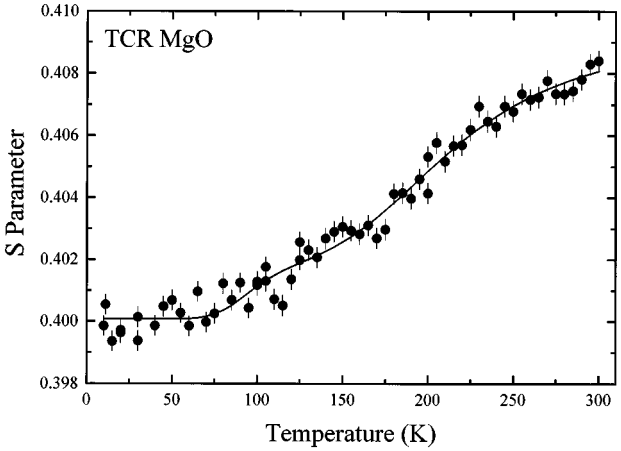

FIG. 5. Parameter S versus temperature for TCR MgO crystals subsequently annealed at 1370 K for 5 min.

ps and 190 ps. In this temperature range an estimate of the mean positron lifetime can be made by

$$\overline{\tau(T)} = P_f \tau_f + P_{st} \tau_{st} + P_v \tau_v . \quad (6)$$

Using the parameters obtained from the fit and $\tau_v = 200$ ps,[2] mean lifetime values of 179−188 ps in the temperature range 100−300 K are obtained from Eq. (6), in reasonable agreement with the observed values.

B. TCR samples

Thermochemical reduction (TCR) of hydrogen-free MgO crystals provides ideal ingredients to study positron trapping at oxygen vacancies. As indicated above, the TCR conditions were extremely severe.[11,12] These conditions produce two main results. First, oxygen vacancies are formed nonstoichiometrically. Second, by virtue of mass action law, cation vacancies (V-type centers) are correspondingly suppressed.

Oxygen vacancies have two charge states, referred to as F^+ and F centers (with one and two electrons, respectively). The optical absorption peaks of both bands coincide at 5.0 eV (250 nm).[19] These vacancies are normally in the F state, unless excited with photons or charged particles, in which case some conversion to F^+ will occur. At any rate, a heat treatment at a moderate temperature (~500 K) will drive the defects completely to the F state without annihilating the vacancies. The atomic concentration of F centers was estimated to be $\sim 10^{-6}$ at^{-1}. Successive anneals at high temperatures in a reducing atmosphere decreased the F concentration (see Table I).

The temperature dependence of the parameter S was measured in a pair of TCR samples prior and after anneals in a reducing atmosphere. This experimental temperature dependence is adjusted to the model discussed in the previous section. Since in TCR samples the only effective positron traps are the neutral F centers, we use a different effective positron trapping rate, given by Eq. (A18) in the Appendix. The model fits very satisfactorily the experimental temperature dependence of S as shown in Fig. 5 for the TCR samples annealed at 1370 K for 5 min. The values of the adjustable parameters are given in Table I. The temperature dependence of the trapping rates κ_{13} and κ_{23}, and the fraction f_{st}, given, respectively, by Eqs. (A15), (A18), and (3), are shown in Fig. 6. Below 60 K no self-trapping is observed. The positron fraction in delocalized states, f_f, is still significant at room temperature ($f_f \sim 8$ %). The trapping rate κ_{23} is essentially temperature independent.

Figure 7 depicts the fractions P_f, P_{st}, and P_v of positrons annihilated at each state. Even though the concentration of F centers is very high, P_f is higher than P_v up to 190 K, indicating that F centers in TCR crystals are much less effective positron traps than V-type centers in as-grown crystals. This would explain why we have never observed trapping saturation in MgO crystals with F center concentrations as high as 10^{-5} at^{-1}.

The lifetime measurements performed on the as-TCR crystals in the temperature range 100−300 K gave two-component spectra with a second lifetime component of ~225 ps attributed to positrons trapped at F centers. Figure

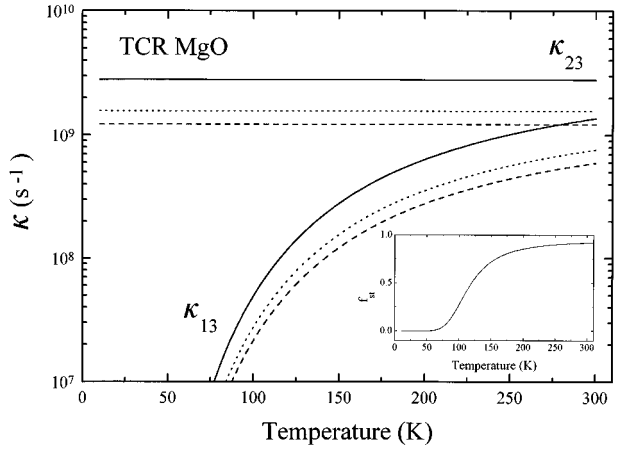

FIG. 6. Trapping rates κ_{13} and κ_{23} versus temperature for TCR MgO crystals: (a) as-TCR (solid line) and after subsequent anneals at (b) 1370 K for 5 min (dotted line), and (c) 1470 K for 10 min (dashed line). The inset shows the variation of the self-trapped positron fraction with the temperature.

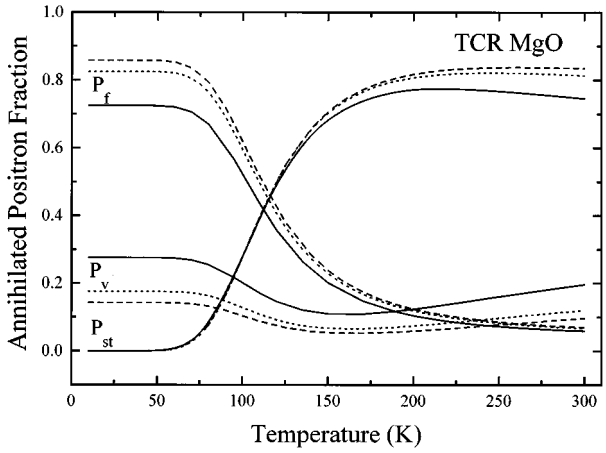

FIG. 7. Fractions of positrons annihilating in delocalized P_f, self-trapped P_{st}, and trapped state P_v versus temperature for TCR MgO: (a) as-TCR (solid line) and after subsequent anneals at (b) 1370 K for 5 min (dotted line), and (c) 1470 K for 10 min (dashed line).

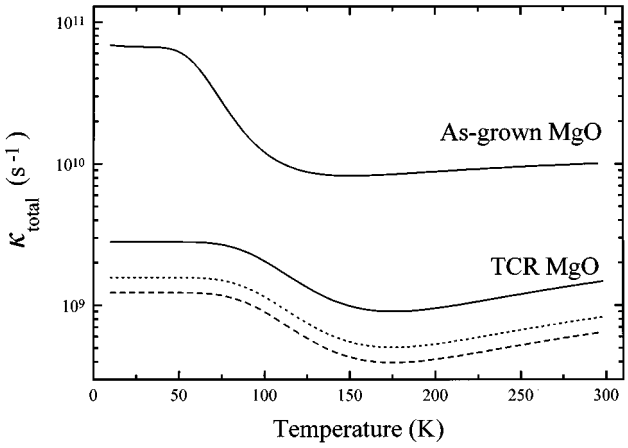

FIG. 9. Total trapping rate $\kappa_{\text{total}}=f_{st}\kappa_{13}+(1-f_{st})\kappa_{23}$ versus temperature for as-grown and TCR MgO. (a) As-TCR (solid line), and after subsequent anneals at (b) 1370 K for 5 min (dotted line) and (c) 1470 K for 10 min (dashed line).

8 shows the experimental temperature dependence of the mean positron lifetime along with the dependence calculated by Eq. (6) using the parameters obtained from the fit of Eq. (5), with $\tau_v=225$ ps.

Lastly, assuming that the total positron trapping rate at defects is $\kappa_{\text{total}}=f_{st}\kappa_{13}+f_f\kappa_{23}$, an apparent positron trapping coefficient μ_{app} can be obtained from the equation $\kappa_{\text{total}}=\mu_{\text{app}}C_v$. Figure 9 shows κ_{total} as a function of temperature for both as-grown and TCR MgO crystals. Using the defect concentration C_v determined by optical absorption measurements, and the f_{st}, κ_{13}, and κ_{23} values given by Eqs. (A15), (A17), and (A18), apparent trapping μ_{app} coefficients at room temperature of $\sim 1\times 10^{16}\text{s}^{-1}$ and $4\times 10^{15}\text{s}^{-1}$ are found for V-type defects and F centers, respectively.

IV. CONCLUSIONS

The temperature dependence of the parameter S in MgO is consistent with the existence of metastable self-trapped positrons above a certain threshold temperature. The energy level of these self-trapped states is $\epsilon=(62\pm 5)$ meV above the energy of the ground delocalized states. The effective activation energy for the hopping process of self-trapped positrons, ΔE, were determined to be (22 ± 2) meV and (52 ± 6) meV for as-grown and TCR samples, respectively; see Table I. This result indicates that the effective energy barrier controlling the thermal hopping of self-trapped positrons depends on the type of defects present in the crystal.

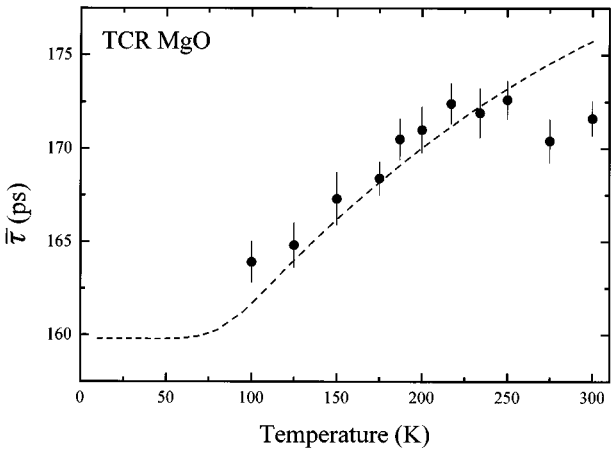

FIG. 8. Mean positron lifetime versus temperature for as-TCR MgO crystals. The dashed curve is the temperature dependence predicted by Eq. (6).

ACKNOWLEDGMENTS

Research at Universidad Carlos III was supported by the Dirección General de Investigación Científica y Técnica of Spain (Project No. PB91-0220) and the Comunidad Autónoma de Madrid (CAM). The research of Y.C. is an outgrowth of past investigations performed at the Oak Ridge National Laboratory.

APPENDIX

This appendix shows the derivation of the mathematical expressions for the fraction of positrons annihilating in delocalized, self-trapped, or trapped states from the three-state trapping model proposed in Sec. III A and represented by the diagram shown in Fig. 2. The rate equations are given by

$$\dot{n}_1(t)=-(\lambda_1+\kappa_{13})n_1(t),$$

$$\dot{n}_2(t)=-(\lambda_2+\kappa_{23})n_2(t), \tag{A1}$$

$$\dot{n}_3(t)=-\lambda_3 n_3(t)+\kappa_{13}n_1(t)+\kappa_{23}n_2(t),$$

where n_i is the positron fraction in the i state, λ_i the annihilation rate, and κ_{ij} the transition rate from the i state to the j state; 1 denotes the metastable self-trapped state, 2 the

delocalized state, and 3 the trapped state at defects. For metastable self-trapping of positrons, the initial conditions to solve Eqs. (A1) are

$$n_1(0)=f_{st}(T),$$
$$n_2(0)=f_f(T)=1-f_{st}(T), \tag{A2}$$
$$n_3(0)=0,$$

according to the discussion of Sec. III A, f_{st} is given by Eq. (3).

Solving the equation system (A1) with the above initial conditions, the positron fraction in the sample, $n(t)$, is given by

$$n(t)=n_1(t)+n_2(t)+n_3(t)$$
$$=I_I e^{-\lambda_I t}+I_{II}e^{-\lambda_{II}t}+I_{III}e^{-\lambda_{III}t}. \tag{A3}$$

Here

$$\lambda_{II}=\lambda_2+\kappa_{23}, \tag{A4}$$

$$\lambda_I=\lambda_1+\kappa_{13}, \tag{A5}$$

$$\lambda_{III}=\lambda_3 \tag{A6}$$

and

$$I_I=f_{st}\frac{\lambda_{III}-\lambda_I+\kappa_{13}}{\lambda_{III}-\lambda_I}, \tag{A7}$$

$$I_{II}=f_f\frac{\lambda_{III}-\lambda_{II}+\kappa_{23}}{\lambda_{III}-\lambda_{II}}, \tag{A8}$$

$$I_{III}=\frac{f_f\kappa_{23}(\lambda_I-\lambda_{III})+f_{st}\kappa_{13}(\lambda_{II}-\lambda_{III})}{(\lambda_{III}-\lambda_I)(\lambda_{III}-\lambda_{II})}. \tag{A9}$$

The fraction of positrons annihilated in each j state will be

$$P_j=\int_0^\infty \lambda_j n_j(t)dt; \quad j=1,\ 2,\ \text{and}\ 3. \tag{A10}$$

Denoting the fraction of positrons annihilated in self-trapped, delocalized, and trapped states by P_{st}, P_f, and P_v, respectively, we have

$$P_{st}\equiv P_1=f_{st}\frac{\lambda_1}{\lambda_1+\kappa_{13}},$$
$$P_f\equiv P_2=f_f\frac{\lambda_2}{\lambda_2+\kappa_{23}}, \tag{A11}$$
$$P_v\equiv P_3=1-P_f-P_{st}.$$

The trapping rates κ_{13} and κ_{23} in Eq. (A11) can be written as

$$\kappa_{13}=\mu_{13}C_v, \tag{A12}$$

$$\kappa_{23}=\mu_{23}C_v, \tag{A13}$$

where μ_{13} and μ_{23} are the effective specific trapping rates per unit concentration for the transitions from the metastable self-trapped to the trapped state, and from the delocalized to the trapped state, respectively. C_v is the temperature-independent atomic concentration of defects.

μ_{13} is governed by the motion of self-trapped positrons through the lattice. According to Seeger,[20] the motion of self-trapped positrons can be treated as a thermally activated hopping process between two adjacent interstitial sites similar to the process described for self-trapped holes in some ionic crystals. Norgett and Stoneham[21] have proposed a temperature dependence for this hopping rate given by

$$\omega_h\propto\sqrt{\frac{1}{kT\Delta E}}\exp\left(\frac{-\Delta E}{kT}\right), \tag{A14}$$

where ΔE is the activation energy for hopping. The effective trapping coefficient μ_{13} is proportional to ω_h. Thus, for κ_{13} we assume the following temperature dependence

$$\kappa_{13}=a\sqrt{\frac{1}{kT\Delta E}}\exp\left(\frac{-\Delta E}{kT}\right), \tag{A15}$$

where a is a constant that contains the defect concentration C_v, the lattice parameter and the matrix element for the transition. The latter is considered to be constant because of the simple symmetry of the MgO lattice.[21]

Next, a temperature dependence for μ_{23} is discussed. Free positron trapping at lattice defects is controlled by two processes: the positron diffusion to the defect and the subsequent transition from the free to the trapped state. For thermalized positrons, steadily distributed in a crystal, the effective specific trapping rate can be expressed as a phenomenological trapping coefficient μ given by[22,23]

$$\mu=\left(\frac{1}{\mu_D}+\frac{1}{\mu_T}\right)^{-1}, \tag{A16}$$

where μ_D and μ_T are the diffusion-limited and transition-limited specific trapping rate, respectively. Thus, we assume $\mu_{23}=\mu$.

Since the positron mobility at low temperature is limited by phonon scattering, according to Seeger[16] the expected temperature dependence for μ_D is $\propto T^{-1/2}$. The temperature dependence of μ_T is determined by the trapping mechanism and the charge state of the defect; to our knowledge, this dependence has not been investigated for vacancies in ionic crystals. For vacancies in metals μ_T is temperature independent. However, this is not the case for wide-band gap materials, because the mechanism of energy transfer depends on the gap width.[24] Calculations in semiconductors indicate that for negative vacancies the temperature dependence of μ_T is $\propto T^{-1/2}$ regardless of the trapping mechanism considered. For neutral vacancies μ_T is temperature independent in wide-gap crystals.[24] These two temperature dependences of μ_T are assumed for negative and neutral vacancies in MgO crystals, i.e., V_{OH}^- centers and F centers, respectively. Using the previously described temperature dependence of μ_D and

μ_T in Eq. (A16), and inserting $\mu_{23}=\mu$ into Eq. (A13), the following temperature dependences are obtained for the trapping rates

$$\kappa_{23}=b+\frac{c}{\sqrt{T}} \tag{A17}$$

for V_{OH}^{-} centers in as-grown MgO crystals, and

$$\kappa_{23}=\frac{de}{d+e\sqrt{T}} \tag{A18}$$

for F centers in TCR MgO crystals. In the latter two equations b, c, d, and e are parameters proportional to the defect concentration C_v.

[1] M.J. Puska, S. Makinen, M. Manninen, and R.M. Nieminen, Phys. Rev. B **39**, 7666 (1989).

[2] R. Pareja, M.A. Pedrosa, and R. González, in *Positron Annihilation*, edited by P.C. Jain, R.M. Singru, and K.P. Gopinathan (World Scientific, Singapore, 1985), p. 708.

[3] R. Pareja, R.M. de la Cruz, M.A. Pedrosa, R. González, and Y. Chen, Phys. Rev. B **41**, 6220 (1990).

[4] M.A. Monge, R. Pareja, R. González, and Y. Chen, Phys. Rev. B **53**, 8950 (1996).

[5] T. Hyodo, J. Kasai, and Y. Takakusa, J. Phys. Soc. Jpn. **49**, 2248 (1980).

[6] J. Kasai, T. Hyodo, and K. Fujiwara, J. Phys. Soc. Jpn. **52**, 3671 (1983).

[7] T. Hyodo and A.T. Stewart, Phys. Rev. B **29**, 4164 (1984).

[8] V.I. Gol'danskii and E.P. Prokop'ev, Sov. Phys. Solid. State **13**, 2481 (1972).

[9] R.M. Nieminen, J. Phys. C **8**, 2077 (1975).

[10] M.M. Abraham, C.T. Butler, and Y. Chen, J. Chem. Phys. **55**, 3752 (1971).

[11] R. González, Y. Chen, and M. Mostoller, Phys. Rev. B **24**, 6862 (1981).

[12] Y. Chen, R. González, O.E. Schow, and G.P. Summers, Phys. Rev. B **27**, 1276 (1983).

[13] R.M. de la Cruz, R. Pareja, A. Segura, V. Muñoz, and A. Chevy, J. Phys. Condens. Matter **5**, 97 (1993).

[14] *American Institute of Physics Handbook*, 3rd ed., edited by Dwight E. Gray (McGraw-Hill, New York, 1982), pp. 4–138.

[15] A.M. Stoneham, in *Theory of Defects in Solids. Electronic Structure of Defects in Insulators and Semiconductors* (Clarendon, Oxford, 1975), p. 664.

[16] A. Seeger, Appl. Phys. **7**, 85 (1975).

[17] Y. Chen and M. M. Abraham, J. Phys. Chem. Solids **51**, 747 (1990).

[18] M.A. Pedrosa, R. Pareja, and R. González, in *Proceedings of the European Meeting on Positron Studies of Defects*, Wernigerode 1987, edited by G. Dlubek, O. Brümmer, G. Brauer, and K. Henning (Martin-Luther Universität, Halle-Wittemberg, 1987), Vol. 2, p. K2.

[19] Y. Chen, J.L. Kolopus, and W.A. Sibley, Phys. Rev. **182**, 962 (1969).

[20] A. Seeger, Appl. Phys. **7**, 257 (1975).

[21] M.J. Norgett and A.M. Stoneham, J. Phys. C **6**, 238 (1973).

[22] A. Seeger, Appl. Phys. **4**, 183 (1974).

[23] K. O. Jensen and A. B. Walker, J. Phys. Condens. Matter **4**, 1973 (1992).

[24] M. Puska, C. Corbel, and R.M. Nieminen, Phys. Rev. B **41**, 9980 (1990).